Cement & Concrete Composites 36 (2013) 101–108

Contents lists available at SciVerse ScienceDirect

Cement & Concrete Composites

journal homepage: www.elsevier.com/locate/cemconcomp

Nano-TiO_2-based architectural mortar for NO removal and bacteria inactivation: Influence of coating and weathering conditions

Ming-Zhi Guo, Tung-Chai Ling, Chi-Sun Poon *

Department of Civil and Structural Engineering, The Hong Kong Polytechnic University, Hung Hom, Kowloon, Hong Kong

ARTICLE INFO

Article history:
Received 2 February 2012
Received in revised form 6 August 2012
Accepted 10 August 2012
Available online 20 August 2012

Keywords:
Titanium dioxide
Photocatalysis
NO removal
Bacteria inactivation
Coating
Weathering

ABSTRACT

In the present study, the photocatalytic activities of TiO_2 dip-coated self-compacting glass mortars (SCGMs), in terms of air pollutant removal and bacteria inactivation, were investigated and compared. TiO_2 dip-coated glass was used as the control to compare performance. Nitrogen oxide (NO) and *Escherichia coli* K12 were used as the target air pollutant and bacteria test strain respectively. In addition, the weathering resistance of TiO_2-coated samples was evaluated. In the case of NO removal, it is clear that no significant difference between TiO_2 dip-coated glass and SCGM was observed, and both exhibited high NO removal efficiency when condition 1 (C1, no weathering) was applied (for EtOH-mortar, up to 14.33 mg m^{-2} h^{-1}). However, after a period of abrasive weathering, condition 3 (C3, abrasive process), the NO removal ability of the TiO_2 dip-coated glass samples almost completely disappeared. In contrast, the NO removal ability of the dip-coated SCGM still remained high (for EtOH-mortar, 8.75 mg m^{-2} h^{-1}). It appears that the porosity of the dip-coated SCGM surface contributed to favourable TiO_2 particles retention after the abrasion action. As for the antibacterial activity, a total inactivation of *E. coli* was observed on the TiO_2 dip-coated glass and SCGM samples within 60 min of UV irradiation. The *E. coli* inactivation of TiO_2 dip-coated glass was nearly negligible after the abrasion process (C3), whereas, the concentration of *E. coli* remaining on the surface of TiO_2 dip-coated SCGM only dropped from about 10^5 to 10^3 CFU/mL. The results suggest that the TiO_2 retained in the porosity of the dip-coated SCGM can still make a contribution to the *E. coli* inactivation. Taking all the results into account, it can be concluded that photocatalytic bacteria inactivation is a more complex process and the results for photocatalytic activity of NO removal cannot always be extrapolated to photocatalytic antibacterial activity.

1. Introduction

Air pollution is a major concern on a global scale. It has been found that poor air quality is responsible for an increased risk of respiratory infections and impaired lung function [1]. Nitrogen oxides (NO_x) generated from various combustion processes are perceived to be one of the principal air pollutants [2]. Recently, the outbreak of scarlet fever in Hong Kong, caused by mutant forms of *Escherichia coli*, has claimed several children's lives. Obviously, poor hygiene conditions in the living environment are mainly to blame. Cement-based materials are used commonly in our living surroundings, such as paving blocks, cement mortars, exterior tiles and concrete. The search for better performing construction and building materials is a never-ending pursuit for researchers and manufacturers around the world. Thanks to advances in photocatalysis science and technology, as well as in nanotechnology, products made with a combination of heterogeneous photocatalysis with building materials have been realized and their popularity has been growing rapidly over the last decade [3–7]. In addition, this photocatalytic cement-based material has been adopted as a promising and effective material to mitigate air pollution.

The advantages of employing cementitious materials as supporting media for the photocatalyst are manifold [8]. Due to their strong binding properties, cementitious materials can immobilize photocatalyst powders within their matrices. Furthermore, the porous structure of the hardened cement pastes helps the incorporated photocatalyst particles to come into bind with the target pollutants to facilitate the photocatalytic conversion. In addition, titanium dioxide (TiO_2) displays the desired properties as an efficient photocatalyst, such as low price, non-toxicity, physical and chemical inertness, and most importantly, high photocatalytic efficiency. A large volume of work has been devoted to the research of TiO_2 induced photocatalysis [9–13], and the mechanisms underlying TiO_2 sensitized heterogeneous photocatalysis are well understood. In general, a TiO_2 mediated photocatalytic reaction can be summarized as follows [6,14]: when TiO_2 is exposed to UV irradiation, it can absorb photons with energies equal to or larger than its band gap (3.2 eV, anatase). Subsequently, electrons (e^-) in the

* Corresponding author. Tel.: +852 2766 6024; fax: +852 2334 6389.
E-mail address: cecspoon@polyu.edu.hk (C.-S. Poon).

0958-9465/$ - see front matter © 2012 Elsevier Ltd. All rights reserved.
http://dx.doi.org/10.1016/j.cemconcomp.2012.08.006

valence band are promoted to the conduction band, leaving positive holes (h^+) in the valence band. The electron–hole pairs may recombine in a short time or further react with pollutants adsorbed on the TiO_2 surface directly or indirectly.

Therefore, at present TiO_2 is the most preferred photocatalyst added to cement-based building materials. From an economical perspective, it could significantly reduce operation and maintenance costs considering that only solar light is required as a driving force to realize its photocatalytic reaction. Up until now, the most intensively studied field of the application of cementitious photocatalytic TiO_2 material is related to air purification, especially for NO_x and VOC removal. Hüsken et al. [15] carried out a comparative analysis of different photocatalytic cementitious products under laboratory conditions. They pointed out that the efficiency with respect to NO_x degradation varied significantly, with some products achieving 40% degradation whereas others showing almost no effect. Hassan et al. [16] investigated the NO_x removal efficiency of different substrate concrete samples with various amounts of TiO_2 before and after laboratory-simulated abrasion and wearing. Interestingly, their results showed that wearing of the specimens with 5% TiO_2 resulted in a small decrease in NO removal efficiency, while the samples with 2% TiO_2 displayed slightly improved NO removal efficiency; however, no explanation was given. The degradation of VOC by photocatalytic cementitious materials has also been demonstrated by several laboratory studies [6,17]. Strini et al. [17] measured the photodegradation of organic compounds (at ppb level) at the surface of photocatalytic materials using a stirred flow reactor with 50% RH and a 100 mL min^{-1} flow. They observed that the photocatalytic activity of pure TiO_2 samples was three to ten times greater than for the cementitious sample prepared with the incorporation of 3% catalyst. The decomposition rate of BTEX was linearly dependent on the concentration of the reactant and the intensity of the irradiation. However, the catalytic activity was not linearly dependent on the TiO_2 content in the samples probably because the formation of catalyst clusters in the cementitious paste was influenced by the different viscosity of the paste. Demeestere et al. [6] studied the potential of using TiO_2 as a photocatalyst in building materials, i.e. roofing tiles and corrugated sheets, for the removal of toluene from air. It was reported that a toluene removal efficiency of 78 ± 2% and an elimination rate of higher than 100 mg h^{-1} m^{-2} were obtained under optimal conditions.

Despite the fact that there is a large volume of work studying the air purification ability of cement-based photocatalytic materials, to our knowledge, few studies have focused on their photocatalytic bacteria inactivation. A detailed investigation is necessary to evaluate the correlation between photocatalytical chemical oxidation and microorganism inactivation.

It also should be noted that the predominantly adopted TiO_2 adding method is intermixing it into various building materials. From a practical perspective, this is understandable considering that this method renders the embedded nano-TiO_2 particles protected by the cementitious materials and can withstand harsh and aggressive environments in which they are put to use. However, the down side is that not all of the initially added TiO_2 particles in the resulting products can be fully exploited (i.e. fulfill their expected photocatalytic activities), because the nano-TiO_2 particles may be encapsulated by the hydration cement products. As a consequence, a significant loss of photocatalytic activity is observed with age. Rachel et al. [18] pointed out that TiO_2–cement mixtures and red bricks containing TiO_2 were significantly less efficient than TiO_2 slurries in decomposing 3-nitrobenzenesulphonic. It is thought that the reduction of active surface and the presence of ionic species, which contribute to the charge recombination, are the reasons for the catalytic activity loss. Lackhoff et al. [19] stated that the carbonation of TiO_2 modified cements lead to a noticeable loss in catalytic efficiency over several months because of the changes in cement surface structure. Recently, our group [20] compared the photocatalytic conversion of nitrogen oxides and toluene removal potentials of TiO_2-intermixed concrete surface layers. The results demonstrated good NO removal but no photocatalytic conversion of toluene was observed. A conclusion drawn from these results is that the transport of photons and surface diffusion of reactants are inhibited by the protective cementitious coatings surrounding the photocatalyst particles in the case of TiO_2-intermixed cement mortar samples. Subsequently, photocatalytic activity is seriously impaired. More recently, our group further studied the photocatalytic activities of nano-TiO_2-intermixed self-compacting glass mortars for NO removal and *E. coli* inactivation. Despite the NO removal ability, no detectable inactivation ability of *E. coli* was observed for all samples under the same UV irradiation. Instead of intermixing TiO_2 into the cementitious materials, Ramirez et al. [21] prepared photocatalytic concrete samples by dip-coating and sol–gel methods and it was found that high toluene degradation efficiencies were obtained on the TiO_2 dip-coated samples.

Based on the information gathered from previous studies, it seems that the method, whereby TiO_2 is added to the substrate materials, plays a vital role in determining the photocatalytic activity of the resulting products. Generally, intermixing TiO_2 into the substrate materials results in a lower photocatalytic activity, while the dip-coating method enables better photocatalytic properties. It is obvious that relatively extensive exposure of the active sites of photocatalysts to the reactants (pollutant) is realized by dip-coating the photo-catalyst onto the substrate materials. Therefore, it raises the question whether the loss of bactericidal ability is due to the significantly reduced photocatalytic activity caused by the intermixing method and whether dip-coating TiO_2 onto mortars realizes photocatalytic antibacterial ability. In the present study, we hope to provide answers to these questions by evaluating and comparing the photocatalytic NO degradation and bacteria inactivation performances of TiO_2-coated glass and mortars, obtained by two different dip-coating methods. Such a comparative study may offer clues about the significance of the TiO_2 addition method and may reveal the critical parameters influencing the associated photocatalytic activity.

2. Experimental details

2.1. Materials and sample preparations

In all the experiments, a commercially available nano-TiO_2 powder (P25, Degussa) was used as the photocatalyst. The particle size of the TiO_2 was 20–50 nm, with a specific BET surface area of 50 ± 15 m^2 g^{-1}. White ordinary Portland cement (WC, TAIHEIYO Cement Corp., Japan) and metakaolin (MK) were used as the cementitious materials. In order to prepare the nano-TiO_2-based architectural cement mortar in this study, a self-compacting-based approach for decorative application was chosen [22,23]. Crushed recycled glass (RG) derived from post-consumer beverage glass was used as fine aggregates in the SCGM. The post-consumer beverage glass used was sourced from a local eco-construction material company. Prior to their experimental use, all the discarded light green glass bottles were washed and then crushed by a mechanical crusher, followed by sieving to a particle size of less than 5 mm.

Self-compacting glass mortars (SCGMs) with 50 MPa compressive strength (28th day) were prepared using a mix proportion of 0.8:0.2:2.0:0.4 (WC:MK:RG:water). In order to investigate the effectiveness of TiO_2 on the photocatalytic activities of the mortar, a 5% (by cementitious mass) dosage of nano-TiO_2 as an addition to the mixture was used. To obtain the targeted mini-slump flow

value of 250 ± 10 mm for self-compacting mortar as per EFNARC [24], an additional 1.14% (by cementitious material mass) of superplasticizer was added. The procedure for the preparation of the SCGM specimens was as follows. First, all the proportioned materials were mixed uniformly for about 5 min using a mechanical mixer. Then the specimens were cast using the self-compacting approach, demoulded and cured in a water tank at a temperature of 27 ± 2 °C for 28 days. For each batch of SCGM, Ø75 × 150 mm cylinder specimens were cut into 10 mm thickness discs using a mechanical diamond saw to examine the photocatalytic activities. Additionally, the porosity of substrate SCGMs was measured based on the ASTM C1202 Vacuum Saturation Method.

Though the TiO_2 dip-coating technique is not appropriate for mortars from a viewpoint of practical applications, the comparison between the dip-coating and intermixing techniques will give a good starting point for further examination of similar systems. In order to prepare the TiO_2 dip-coated glass and SCGM, two methods were adopted. The substrate materials were first cleaned by sonication in acetone, ethanol and distilled deionized water (DDW) for 30 min, respectively. In the first TiO_2-coating technique, the substrate materials were dip-coated with a TiO_2 film. The TiO_2 suspension was prepared from a 25 g/L P25 ethanol suspension with the addition of 25 g/L glycerol. The prepared suspension was stirred for 15 min, before the substrate materials were dipped into it (for 5 min). After that, the TiO_2-coated glass (EtOH-glass) and SCGM (EtOH-mortar) were calcinated at 450 °C for 120 min to burn off the organic materials so that the TiO_2 film could be bonded to the substrates.

It is known that high temperature has a negative impact on cement-based mortar. Besides, from an economic perspective and for easy manipulation, another coating method, capable of being performed at a lower temperature, was adopted. First, a suspension of methanol and P25 (25 g/L) was prepared. Afterwards, the glass (MeOH-glass) and/or mortar (MeOH-mortar) were dipped into the suspension for 5 min, followed by oven-drying at 60 °C for 120 min. The sample IDs and experiment testing descriptions are listed in Table 1.

2.2. Weathering conditions for TiO_2-coated samples

TiO_2 dip-coated samples were subjected to three different weathering conditions (Table 2). Condition 1(C1) comprised normal (control) weathering conditions under which no additional treatment was applied to the samples. In condition 2 (C2), all the samples were washed using 500 mL of deionized water at a time to simulate raining conditions. The samples were positioned at an inclined angel of 45° and the deionized water was allowed to run over them. The "raining" cycle was repeated 10 times. Following this, condition 3 (C3), an abrasive process, was applied to all the samples. In this process, a wet cotton towel was used to scrape the surface containing the TiO_2 layer by a manually applied back and forth motion for 20 cycles to simulate wearing of the nano-TiO_2 coating layer. The photo-catalytic activities of the samples (NO removal and antibacterial abilities) were examined before and immediately after each weathering process.

2.3. Bacterial strains and culture conditions

A UV-resistant *E. coli* K12 was used as the test strain in this study, which is a gram-negative bacterium widely selected as a model microorganism in many photocatalytic bactericidal experiments.

E. coli K12 was sub-cultured and maintained on nutrient agar plates. To prepare the bacterial cultures for the experiment, single colonies were isolated from the nutrient broth agar plate cultures and used to inoculate 50 mL of the nutrient broth liquid media (pH 7) in a 250 mL flask. Then the flask was incubated at 37 °C for 18 h in an orbital incubator set at 150 rpm. To eliminate broth medium, the cells were harvested by centrifugation at 4000 rpm for 5 min. After this, the treated cells were washed, re-suspended and diluted to the targeted concentration of about 1×10^5 colony forming units (CFU)/mL in sterilized 0.9% (w/v) sodium chloride solution. All the equipment and materials were autoclaved at 121 °C for 15 min before the experiment to ensure sterility.

2.4. Photocatalytic conversion of NO

2.4.1. Reactor setup

The reactor was made according to the specifications of JIS R1701-1 with slight modifications. The dimension of the reactor was 700 mm in length, 400 mm in width and 130 mm in height. Testing samples were placed on a rack at the centre of the reactor. Two UV-A fluorescent lamps (TL 8W/08 BLB, Philips, Holland) were positioned parallel to each other on the glass cover of the reactor to provide UV radiation. The wavelength of the lamps ranged from 300 to 400 nm with a maximum intensity at 365 nm. The distance between the lamps and the reactor was adjusted to achieve the required intensity. The UV intensity was measured by a digital radiometer equipped with a DIX-365A UV-A sensor (Spectroline DRC-100X, Spectronics Corporation, USA). A zero air generator (Thermo Environmental Inc. Model 111) was used to supply a constant clean air flow. The testing gas was a mixture of zero air and standard NO (Arkonic Gases, Hong Kong). The humidity in the reactor was controlled by passing the zero air stream through a humidification chamber. The NO concentration was continuously measured using a Chemilluminescence NO analyzer (Thermo Environmental Instruments Inc. Model 42c, USA). A thermometer, a humidity sensor and an adjustable rack supporting the specimens were placed inside the reactor. The reactor was completely sealed with no detectable leakage. A schematic diagram of the experimental setup for this study is shown in Fig. 1.

2.4.2. Testing protocol

All experiments were carried out at ambient temperature (25 ± 3 °C). The flow of the testing gas (1000 ppb NO) was adjusted by two flow controllers to a rate of 3 L min^{-1} and the relative humidity (RH) was controlled at 50 ± 5%. The UV intensity was 10 W m^{-2} at the centre of the reactor. Prior to all photocatalytic conversion processes, the testing gas stream was introduced to the reactor in the absence of UV radiation for at least half an hour to obtain the desired RH as well as gas–solid adsorption–desorption

Table 1
Samples prepared for NO removal and bacteria inactivation tests.

Sample ID	Description
Mortar without TiO_2	Self-compacting glass mortar (SCGM) without TiO_2
Mortar with 5% TiO_2	Self-compacting glass mortar (SCGM) intermixed with 5%TiO_2 (by cementitious mass)
Glass	Reference glass without TiO_2 coating
EtOH-glass	Glass dip-coated with TiO_2 suspended in ethanol and glycerol solution, calcinated at 450 °C for 120 min
MeOH-glass	Glass dip-coated with TiO_2 suspended in methanol solution, oven-dried at 60 °C for 120 min
EtOH-mortar	Mortar dip-coated with TiO_2 suspended in ethanol and glycerol solution, calcinated at 450 °C for 120 min
MeOH-mortar	Mortar dip-coated with TiO_2 suspended in methanol solution, oven-dried at 60 °C for 120 min

Table 2
Three different weathering conditions.

Weathering condition	Description
Condition 1 (C1)	A normal (control) weathering condition with no additional treatment
Condition 2 (C2)	Rain simulating condition in which samples were washed by deionized water (500 mL for 10 cycles)
Condition 3 (C3)	Wearing simulating condition in which samples were scraped by of a wet towel applied manually (20 cycles)

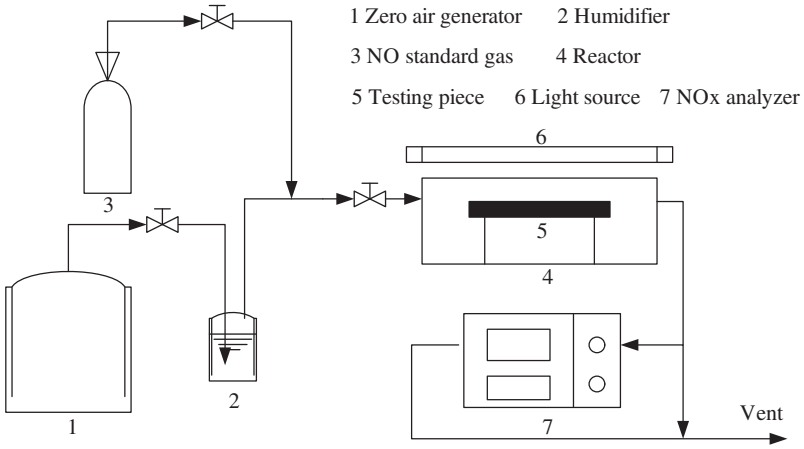

Fig. 1. Schematic diagram of NO removal experimental setup.

equilibrium. Then the UV lamps were turned on for the photocatalysis process to begin. For each sample the NO removal test lasted for 60 min and the concentration change of NO and NO_2 at the outlet was recorded. Due to the small amount of NO_2 generation (less than 30 ppb in all tests), the photocatalytic ability of the samples was expressed by NO reduction. Every sample was tested three times and the average value together with the standard deviation was reported. The calculation of the amount of NO removal, following the instructions in JIS R 1701-1, is shown below:

$$Q_{NO} = \frac{f}{(22.4)} \int ([NO]_0 - [NO])_{dt}$$

where Q_{NO} is the amount of nitrogen monoxide removed by the test sample (μmol); $[NO]_0$ is the inlet concentration of nitrogen monoxide (ppm); $[NO]$ is the outlet concentration of nitrogen monoxide (ppm); t is the time of removal operation (min); f is the flow rate converted into that at the standard state (0 °C, 1.013 kPa) (L min^{-1})

The specific NO removal in units of mg h^{-1} m^{-2} is calculated by the following formula:

$$\theta = \frac{Q_{NO} \times MW_{NO} \times 10^3}{Sampling \cdot time(h) \times Surface \cdot area(m \times m)}$$

where θ is the specific photoactivity (mg h^{-1} m^{-2}); Q_{NO} is the amount of nitrogen monoxide removed by the test sample (mol); MW_{NO} is the molecular weight of *NO*

2.5. Photocatalytic inactivation of bacteria

One milliliter of *E. coli* K12 cell suspension was pipetted onto each of the prepared glass and mortar samples, which were then placed in sterilized Petri dishes to prevent drying (Fig. 2). The Petri dishes with the testing sample were subject to illumination by the same UV lamps used in the NO removal experiments. The light intensity striking the surface of testing samples was 10 Wm^{-2}. The cell suspension was collected by washing the sample with 20 mL 0.9% sodium chloride solution at different time intervals of 20, 40, 60, 90 and 120 min, respectively, after the irradiation. Then

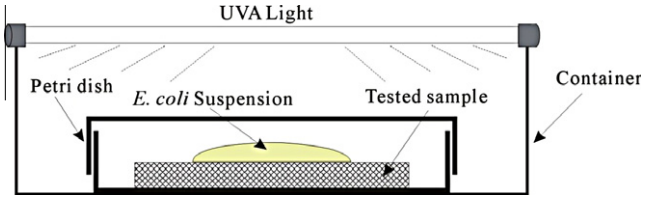

Fig. 2. Schematic diagram of bacterial inactivation experimental setup.

serial dilutions of the collected cells suspension were appropriately performed, and 100 μL of diluted suspension was spread on the nutrient agar plate and incubated at 37 °C for 18 h. Three replicated plates were used for each incubation to verify the reproducibility of the results. The loss of viability was examined by the viable count of the colony forming units on the plates. In all the experiments, negative control tests under conditions of darkness and positive controls only for UVA were carried out simultaneously.

3. Results and discussion

3.1. Photocatalytic NO removal and bacterial inactivation of nano-TiO_2 dip-coated samples

Fig. 3 displays the photocatalytic NO removal of the different tested samples. It is clear that the photocatalytic NO removal activity of all TiO_2-coated materials, without undergoing weathering conditions (C1), was proved to be significantly improved by the use of dip-coating methods. The amount of NO removed by the TiO_2 dip-coated SCGM (EtOH-mortar) was about 14 mg h^{-1} m^{-2}, which outperformed that of the 5% TiO_2-intermixed SCGM. According to the differences in NO removal between TiO_2-intermixed and dip-coated samples, the dip-coating method seemed to provide the substrate materials more active sites, which facilitated the surface reactions.

It also can be seen that the substrate materials, as well as the two TiO_2 dip-coating methods, had a negligible effect on NO

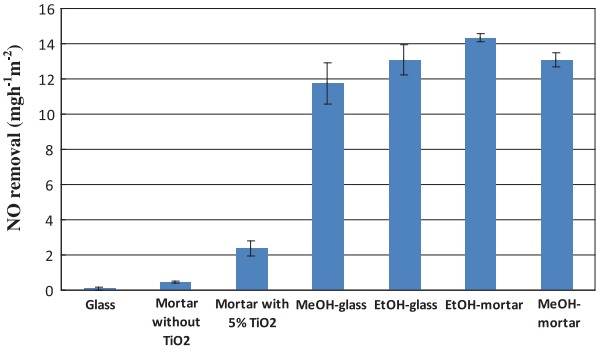

Fig. 3. Comparison of NO removal of different samples under 60 min UV irradiation.

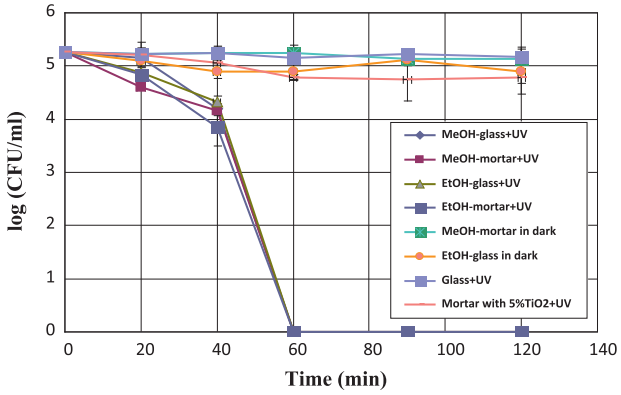

Fig. 5. Photocatalytic inactivation of *E. coli* of different samples subject to two different conditions.

removal activity. Fig. 4 shows the photocatalytic NO removal profile of 5% TiO_2-intermixed SCGM and the TiO_2 dip-coated SCGM. It is evident that a significantly enhanced NO removal activity occurred on TiO_2-coated SCGM (MeOH-mortar). However, it is interesting to note that as the reaction proceeded, the amount of NO removed by MeOH-mortar gradually decreased, whereas this was not observed for the 5% TiO_2-intermixed SCGM. This phenomenon has been referred to as the deactivation of the catalyst and encountered by many researchers [25,26]. This could be attributed to the generation of reaction intermediates, which unfavourably occupy the active sites on the catalyst surface [27]. It is possible that for the dip-coated samples, more active sites were exposed to the reactants leading to higher deactivation as suggested by the above results.

Given the significant increase in photocatalytic activity of the TiO_2 dip-coated materials for NO degradation, it is reasonable to expect that their corresponding bacteria inactivation can also be improved. This assumption is supported by the results of bacteria inactivation of the TiO_2 dip-coated samples demonstrated in Fig. 5. It can be seen that there was complete inactivation of *E. coli* within 60 min of UV irradiation on all the samples dip-coated with TiO_2 regardless of different substrate and dip-coating method. Neither the SCGM intermixed with 5% TiO_2 exposed to 120 min of UV irradiation nor TiO_2-coated samples in the dark showed any detectable bactericidal effects for *E. coli*. It should be noted that the survival curve did not follow a simple single exponential decay process as a function of illumination time, as is often the case in chemical oxidation. It is clear that the initial photocatalytic inactivation step was slow, after which the bacterial inactivating process was faster. This is consistent with a previous study by Sunada et al. [28]. They reported that the photokilling of *E. coli* consisted of two stages: an initial slower rate step followed by a higher one. It is well-known that the cell wall and cytoplasmic membrane are the initial targets of photocatalysis-generated reactive oxygen species (ROS). Because of the complex structure of these initial targets, this process requires a certain amount of cumulative damage and involves many more radicals [29,30]. Therefore, the first step takes a relatively long time and leads to an apparent delay in the bacteria inactivation profiles. When the oxidative damage is sufficient to destroy the cell wall and membrane, intracellular contents start to flow rapidly out of the cells. Eventually, this results in a quick loss of cell viability.

In conclusion, it has been clearly demonstrated that dip-coating TiO_2 onto the samples contributed to high photocatalytic activity. Not only did an expected increase in the efficiency of NO removal occur, but a total inactivation of *E. coli* was also observed. It seems that the dip-coating method resulted in many more active sites on the surface of the substrate materials available for the photocatalytic reaction. As a result, instead of recombination, the photo-generated electrons and holes could more easily react with oxygen

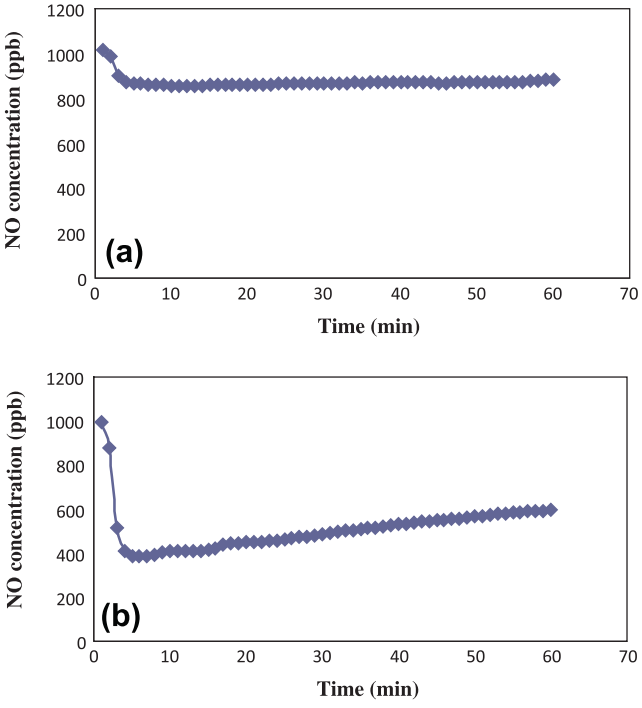

Fig. 4. Photocatalytic NO removal profile of (a) mortar with 5% TiO_2 and (b) MeOH-mortar during a course of 60 min UV irradiation.

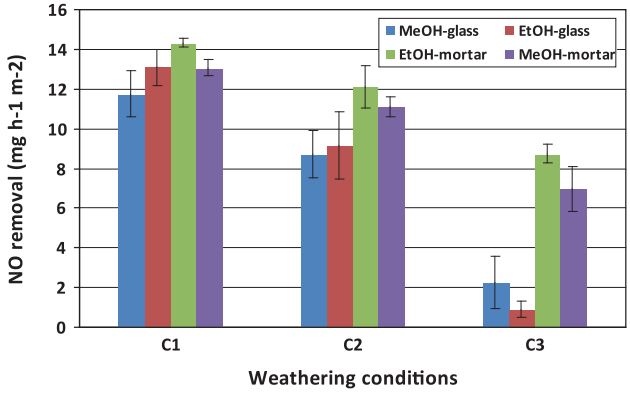

Fig. 6. Changes of NO removal activity of TiO_2 dip-coated samples under 60 min UV irradiation subject to three different weathering conditions.

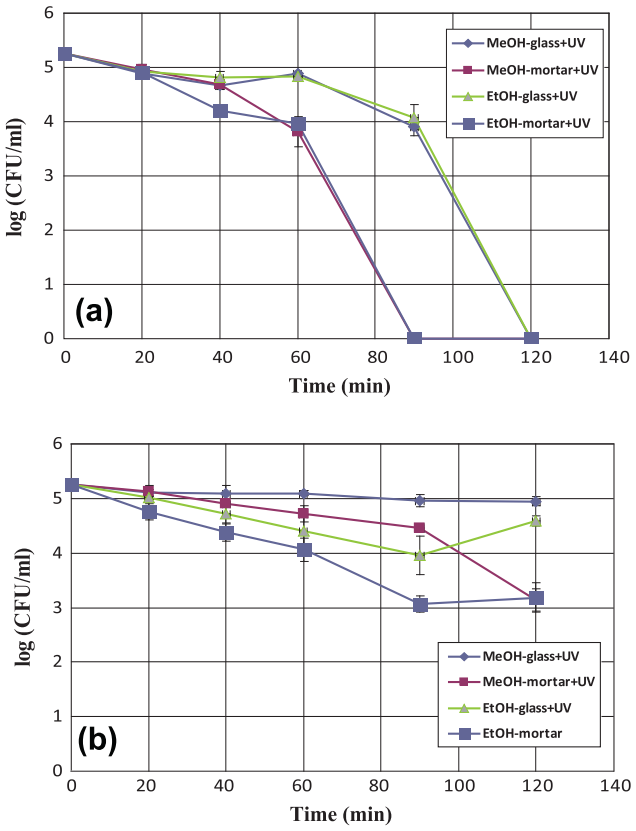

Fig. 7. Changes of photocatalytic bacteria inactivation of TiO_2 dip-coated samples under 120 min UV irradiation after two different weathering conditions: (a) condition 2 (C2) and (b) condition 3 (C3).

and/or water to form highly reactive species, which were instantly consumed by reactants adsorbed on the surface of substrate materials. Therefore, the TiO_2 dip-coated materials exhibited a much higher photocatalytic activity in comparison to TiO_2-intermixed mortars.

Another interesting aspect of the results was the photoinduced hydrophilicity on the surface of TiO_2 dip-coated samples. In fact, this photocatalytic phenomenon has long been discovered and intensively studied, and the underlying mechanism is well understood [9,31]. Owing to the photoinduced hydrophilicity, the bacterial suspensions were found to spread more extensively (by visual observation) across the surface when compared with that of the 5% TiO_2-intermixed mortar. As a consequence, total inactivation of bacteria took place within a relatively short period (60 min). Thus, the bacteria inactivation activity on the surface of TiO_2 dip-coated samples is believed to be the result of the synergetic effects of photocatalytic oxidation and photoinduced hydrophilicity.

3.2. Durability of TiO_2 dip-coated samples

When condition 2 (C2) was applied, under which samples were only washed using water without imposing any abrasion, a decrease in NO removal ability was observed for all the samples. The amount of NO removed by TiO_2-coated samples dropped from 11.75 to 8.73 mg h^{-1} m^{-2} for MeOH-glass, from 13.09 to 9.15 mg h^{-1} m^{-2} for EtOH-glass, from 14.33 to 12.14 mg h^{-1} m^{-2} for EtOH-mortar and from 13.06 to 11.11 mg h^{-1} m^{-2} for MeOH-mortar, respectively (Fig. 6). It is apparent that the loss of photocatalytic NO removal of the TiO_2-coated glass samples was slightly higher (17–26%) than that of TiO_2-coated SCGM regardless of the dip-coating method used. With respect to bacteria inactivation, a similar reduction in bactericidal ability was observed for each TiO_2-coated glass and SCGM after undergoing condition 2. The time required for total bacteria inactivation was 120 min for the TiO_2-coated glass and 90 min for the TiO_2-coated SCGM respectively (Fig. 7a). Both were longer than that of samples under condition 1 (C1). It seems that the substrate materials, other than dip-coating methods, had a major impact on photocatalytic activity when the samples were subjected to weathering conditions.

This impact was much more obvious when abrasive condition 3 (C3) was applied to all the TiO_2-coated samples. It is clear that after undergoing condition 3, all the TiO_2 dip-coated glass samples almost totally lost their photocatalytic NO removal ability, 2.25 mg h^{-1} m^{-2} for MeOH-glass and 0.90 mg h^{-1} m^{-2} for EtOH-glass, respectively, whereas photocatalytic NO removal remained relatively high for TiO_2-coated SCGM, 8.75 mg h^{-1} m^{-2} for EtOH-mortar and 6.97 mg h^{-1} m^{-2} for MeOH-mortar, respectively (Fig. 6). It is noteworthy that even when subjected to highly abrasive conditions (C3), the NO removal ability of TiO_2-coated SCGM was still much higher than that of 5% TiO_2-intermixed SCGM.

On the other hand, after being subjected to condition 3, total photocatalytic inactivation of *E. coli* was no longer observed for all the samples even after 120 min of UV irradiation (Fig. 7b). Nonetheless, it should be noted that the concentration of *E. coli*

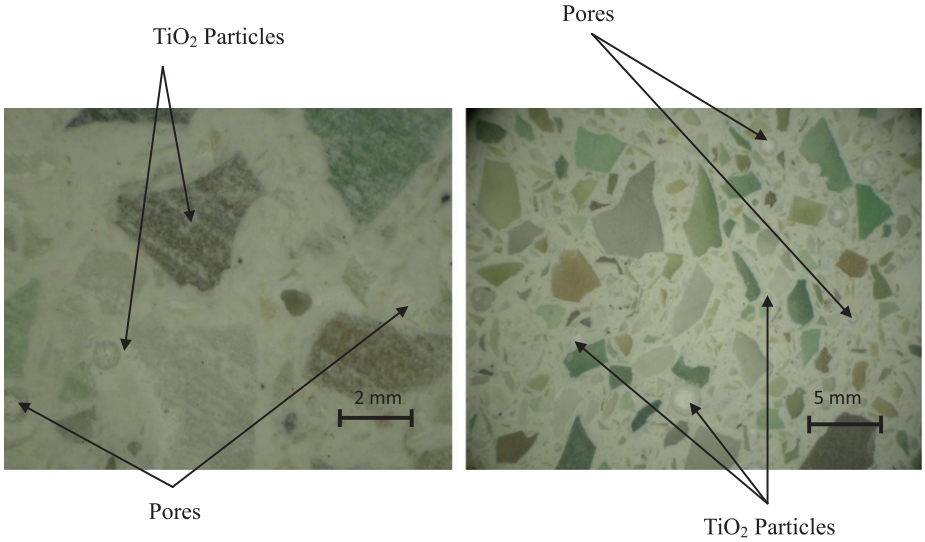

Fig. 8. Macrographs of MeOH-mortar showing TiO_2 particles within pores: (a) under condition 1 (C1) and (b) after condition 3 (C3).

Table 3
Porosity of the substrate samples.

Material	Porosity (%)
Glass	~0
Mortar without TiO_2	14.8 ± 0.4
Mortar with 5%TiO_2	15.0 ± 0.8

remaining on the surface of the TiO_2 dip-coated SCGM dropped from approximately 10^5–10^3 CFU/mL.

Considering all the results of the weathering resistance experiment, the TiO_2 dip-coated SCGM samples were superior to the TiO_2 dip-coated glass with regard to withstanding abrasion. This may be due to substrate roughness and porosity playing a positive role in the retention of TiO_2 particles on the substrate surface (Fig. 8). When the TiO_2 dip-coated SCGM was subjected to highly abrasive conditions (C3), it is likely that the surface porosity (with total water porosity at about 15.0%) and rough texture of the SCGM (see Table 3) help to retain the TiO_2 coatings during the weathering process as the TiO_2 particles that have been deposited in the pores of mortars are not removed. On the other hand, the smooth surface (0% porosity) of the glass was more prone to losing the TiO_2 coatings. Therefore, compared with the TiO_2-coated glass, relatively high photocatalytic activity was preserved on the TiO_2-coated SCGM. Actually, these findings are consistent with the results of Ramirez et al. [21] who found that high porosity and roughness values were favourable for retaining more TiO_2 particles for toluene removal.

It is important to note that after a period of abrasive weathering (C3), NO removal ability still remained high, comparable to that of the TiO_2 dip-coated glass samples undergoing condition 2. However, this did not translate into total bacteria inactivation, as was the case for the TiO_2 dip-coated glass samples subjected to condition 2. It is likely that the TiO_2 particles dominating the surface of the mortars, which were mostly wiped off during abrasion, were mainly responsible for bacteria inactivation. But the remaining TiO_2 particles, mainly in the pores of mortars, were responsible for NO removal and given that there was an observable decrease in the concentration of *E. coli* on the TiO_2 dip-coated SCGM, it is possible that the TiO_2 particles retained in the pores could still have been playing a minor role in the inactivation of *E. coli*. Considering that the concentration of bacteria in air is much lower than that used in the experiment, this reduced bacteria inactivation ability could still effectively inhibit the growth of bacteria in contact with the surface of the TiO_2 dip-coated mortars.

4. Conclusions

The NO removal and bacteria inactivation of TiO_2 dip-coated materials were assessed and compared. By dip coating TiO_2 onto the surface of glass and SCGM, significantly enhanced NO removal activity accompanied by total inactivation of *E coli* within a relatively short time (60 min) was detected, suggesting that the two different dip-coating methods could be used to prepare cement-based substrate materials with high photocatalytic activities. After undergoing the abrasion weathering condition (C3), TiO_2 dip-coated glass samples almost completely lost NO removal ability, whereas, the TiO_2 dip-coated SCGM still exhibited high NO removal activity, which was even higher than that of the samples prepared by intermixing 5% TiO_2 into the cement mortars. There was still an observable decrease in the concentration of *E. coli* on the TiO_2 dip-coated SCGM. The results indicated that the high porosity of the dip-coated SCGM surface was mainly responsible for the favourable TiO_2 particles retention, and that the TiO_2 retained in the pores of the SCGM still could contribute to *E. coli* inactivation.

It can further be concluded that bacteria inactivation is a more complex process requiring a certain amount of ROS accumulation compared with photocatalytic NO removal activity. According to the results of this study, the photocatalytic activity of NO removal cannot always be extrapolated to photocatalytic activity of bacteria inactivation despite a certain limited correlation existing between the two processes. Furthermore, the way in which TiO_2 is incorporated into the substrate, as well as the characteristics of the substrate materials have an important impact on the photocatalytic efficiency of the produced photocatalytic material. The former plays a decisive role in determining subsequent photocatalytic activity, while the latter has proved to be a key factor influencing weathering resistance. In the present study, the TiO_2 dip-coated self-compacting SCGM displayed relatively high photocatalytic efficiency in both NO removal and bacteria inactivation, and could endure high abrasive weathering conditions.

Acknowledgements

The authors wish to thank the Environment and Conservation Fund, and The Hong Kong Polytechnic University for funding support.

References

[1] Hessisches landesamt für umwelt und geologie. Stickstoffdioxid (NO_2) Quellen-emissionen-auswirkungen auf gesundheit und ökosystem-bewertungen-immissionen. <http://www.hlug.de>.
[2] Ballari MM, Yu QL, Brouwers HJH. Experimental study of the NO and NO_2 degradation by photocatalytically active concrete. Catal Today 2011;161:175–80.
[3] Kaneko M, Okura I. Photocatalysis-science and technology. Kodansha Springer; 2002.
[4] Sanchez F, Sobolev K. Nanotechnology in concrete – a review. Constr Build Mater 2010;24:2060–71.
[5] Pacheco-Torgal F, Jalali S. Nanotechnology: advantages and drawbacks in the field of construction and building materials. Constr Build Mater 2011;25:582–90.
[6] Demeestere K, Dewulf J, De Witte B, Beeldens A, Van Langenhove H. Heterogeneous photocatalytic removal of toluene from air on building materials enriched with TiO_2. Build Environ 2008;43:406–14.
[7] Ruot B, Plassais A, Olive F, Guillot L, Bonafous L. TiO_2-containing cement pastes and mortars: measurements of the photocatalytic efficiency using a rhodamine B-based colourimetric test. Sol Energy 2009;83:1794–801.
[8] Chen J, Poon CS. Photocatalytic cementitious materials: influence of the microstructure of cement paste on photocatalytic pollution degradation. Environ Sci Technol 2009;43:8948–52.
[9] Fujishima A, Rao TN, Tryk DA. Titanium dioxide photocatalysis. J Photoch Photobiol C 2000;1:1–21.
[10] Chen XB, Mao SS. Titanium dioxide nanomaterials: synthesis, properties, modifications, and applications. Chem Rev 2007;107:2891–959.
[11] Fujishima A, Zhang XT, Trylc DA. TiO_2 photocatalysis and related surface phenomena. Surf Sci Rep 2008;63:515–82.
[12] Leary R, Westwood A. Carbonaceous nanomaterials for the enhancement of TiO_2 photocatalysis. Carbon 2011;49:741–72.
[13] Henderson MA. A surface science perspective on TiO_2 photocatalysis. Surf Sci Rep 2011;66:185–297.
[14] Chen J, Poon CS. Photocatalytic construction and building materials: from fundamentals to applications. Build Environ 2009;44:1899–906.
[15] Hüsken G, Hunger M, Brouwers HJH. Experimental study of photocatalytic concrete products for air purification. Build Environ 2009;44:2463–74.
[16] Hassan MM, Dylla H, Mohammad LN, Rupnow T. Evaluation of the durability of titanium dioxide photocatalyst coating for concrete pavement. Constr Build Mater 2010;24:1456–61.
[17] Strini A, Cassese S, Schiavi L. Measurement of benzene, toluene, ethylbenzene and o-xylene gas phase photodegradation by titanium dioxide dispersed in cementitious materials using a mixed flow reactor. Appl Catal B Environ 2005;61:90–7.
[18] Rachel A, Subrahmanyam M, Boule P. Comparison of photocatalytic efficiencies of TiO_2 in suspended and immobilised form for the photocatalytic degradation of nitrobenzenesulfonic acids. Appl Catal B Environ 2002;37:301–8.
[19] Lackhoff M, Prieto X, Nestle FD, Niessner R. Photocatalytic activity of semiconductor-modified cement – influence of semiconductor type and cement ageing. Appl Catal B Environ 2003;43:205–16.
[20] Chen J, Kou SC, Poon CS. Photocatalytic cement-based materials: comparison of nitrogen oxides and toluene removal potentials and evaluation of self-cleaning performance. Build Environ 2011;46:1827–33.

[21] Ramirez AM, Demeestere K, De Belie N, Mantyla T, Levanen E. Titanium dioxide coated cementitious materials for air purifying purposes: preparation, characterization and toluene removal potential. Build Environ 2010;45:832–8.
[22] Ling TC, Poon CS, Kou SC. Feasibility of using recycled glass in architectural cement mortar. Cem Concr Comp 2011;33:848–54.
[23] Ling TC, Poon CS. Properties of architectural mortar prepared with recycled glass with different particle sizes of recycled glass. Mater Des 2011;32:2675–84.
[24] EFNARC. Specification and guidelines for self-compacting concrete. European federation for specialist construction chemicals and concrete system. English ed., Norfolk, UK; February 2002.
[25] Obee TN, Brown RT. TiO_2 photocatalysis for indoor air applications: effects of humidity and trace contaminant levels on the oxidation rates of formaldehyde, toluene and 1,3-butadiene. Environ Sci Technol 1995;29:1223–31.
[26] Cao L, Gao Z, Suib SL, Obee TN, Hay SO, Freihaut JD. Photocatalytic oxidation of toluene on nanoscale TiO_2 catalysts: studies of deactivation and regeneration. J Catal 2000;196:256–61.
[27] Zhao J, Yang XD. Photocatalytic oxidation for indoor air purification: a literature review. Build Environ 2003;38:645–54.
[28] Sunada K, Watanabe T, Hashimoto K. Studies on photokilling of bacteria on TiO_2 thin film. J Photochem Photobiol A Chem 2003;156:227–33.
[29] Marugan J, Grieken RV, Pablos C, Sordo C. Analogies and differences between photocatalytic oxidation of chemicals and photocatalytic inactivation of microorganisms. Water Res 2010;44:789–96.
[30] Marugán J, Van Grieken R, Sordo C, Cruz C. Kinetics of the photocatalytic disinfection of *Escherichia coli* suspensions. Appl Catal B Environ 2008;82:27–36.
[31] Wang R, Hashimoto K, Fujishima A, Chikuni M, Kojima E, Kitamura A, et al. Light-induced amphiliphilic surface. Nature 1997;388:431–2.